

ORIGINAL

Design and Comparison of Controllers for a Robotic Transfemoral Prosthesis

Diseño y Comparación de Controladores para una Prótesis Transfemoral Robótica

Guillermo Mosquera¹ , Vladimir Bonilla¹ , Sofía Vergara² , Christian Rueda¹ , Marcelo Moya¹ 

¹Universidad Internacional del Ecuador UIDE, Facultad de Ciencias Técnicas. Quito, Ecuador.

²MECUADOR. Quito, Ecuador.

Cite as: Mosquera G, Bonilla V, Vergara S, Rueda C, Moya M. Design and Comparison of Controllers for a Robotic Transfemoral Prosthesis. Data and Metadata. 2025; 4:759. <https://doi.org/10.56294/dm2025759>

Submitted: 08-05-2024

Revised: 11-09-2024

Accepted: 29-03-2025

Published: 30-03-2025

Editor: Dr. Adrián Alejandro Vitón Castillo 

Corresponding Author: Guillermo Mosquera 

ABSTRACT

This study investigates the performance of four control strategies—Proportional-Derivative (PD), Feedforward-Feedback PD (FF-FB PD), Linear Quadratic Regulator (LQR), and Feedforward-Feedback LQR (FF-FB LQR)—implemented on a robotic transfemoral prosthesis. The performance metrics, including overshoot, settling time, trajectory tracking accuracy, and torque requirements, were evaluated using simulation models. The results indicate that the FF-FB LQR controller demonstrated superior performance, achieving the lowest overshoot (4,98 %) and near-zero trajectory tracking error. All controllers required approximately 8,6 Nm of torque, suggesting consistent energy requirements across strategies despite their performance differences. The LQR controller exhibited the best stability, minimizing overshoot and improving overall system response. These findings highlight the advantages of feedforward-feedback control strategies, particularly the FF-FB LQR, for controlling robotic transfemoral prostheses with enhanced stability and accuracy.

Keywords: Proportional-Derivative (PD) Controller; Linear Quadratic Regulator (LQR) Controller; Two Degrees of Freedom Controller; Transfemoral Prosthesis.

RESUMEN

Este estudio investiga el rendimiento de cuatro estrategias de control—Proporcional-Derivativo (PD), PD con realimentación anticipada (FF-FB PD), Regulador Cuadrático Lineal (LQR) y LQR con realimentación anticipada (FF-FB LQR)—implementadas en una prótesis robótica transfemoral. Se evaluaron los parámetros de rendimiento, incluidos el sobreimpulso, el tiempo de estabilización, la precisión del seguimiento de trayectoria y los requerimientos de torque, utilizando modelos de simulación. Los resultados indican que el controlador FF-FB LQR mostró un rendimiento superior, logrando el menor sobreimpulso (4,98 %) y un error casi nulo en el seguimiento de trayectoria. Todos los controladores requirieron aproximadamente 8,6 Nm de torque, lo que sugiere requerimientos de energía consistentes entre las estrategias, a pesar de las diferencias en rendimiento. El controlador LQR exhibió la mejor estabilidad, minimizando el sobreimpulso y mejorando la respuesta general del sistema. Estos hallazgos destacan las ventajas de las estrategias de control con realimentación anticipada, particularmente el FF-FB LQR, para controlar prótesis robóticas transfemorales con mayor estabilidad y precisión.

Palabras clave: Controlador Proporcional-Derivativo (PD); Controlador Regulador Cuadrático Lineal (LQR); Controlador de Dos Grados de Libertad; Prótesis Transfemoral.

INTRODUCTION

The development of transfemoral prostheses is crucial given the increasing number of individuals with lower-limb amputations. In Ecuador, data from the Consejo Nacional para la Igualdad de Discapacidades (CONADIS) up to September 2023 indicates that there are 215,706 registered individuals with disabilities, with 44,87 % of these individuals having physical disabilities, a significant portion of whom are lower-limb amputees.⁽¹⁾

Within this group, many amputees fall within the working-age population (18 to 65 years), accounting for 61,34 % of the total disabled population.⁽¹⁾ This emphasizes the socio-economic importance of developing effective prosthetic solutions that enable these individuals to regain functional independence and continue contributing to the labor market. A significant challenge in the prosthesis field is the creation of cost-effective solutions that meet the needs of a population with diverse levels of disability, as 48,96 % of individuals fall within the 30 % to 49 % disability range, while 32,64 % experience 50 % to 74 % disability.⁽¹⁾

Globally, the World Health Organization (WHO) estimates that more than 30 million people require prosthetic or orthotic services, with this number expected to increase due to non-communicable diseases, trauma, and diabetes.⁽²⁾ In developing nations such as Ecuador, access to high-quality, affordable prosthetics is often limited, impacting amputees' mobility, social participation, and economic productivity. The high demand for prosthetics, coupled with limited resources, highlights the need for innovative designs that are affordable and sustainable in low-income settings.⁽²⁾

The need for transfemoral prostheses, or prostheses for individuals with above-knee amputations, is influenced by a wide range of factors, including trauma, disease, and other medical conditions. Amputation often results from conditions such as diabetes or traumatic injuries, which impact a significant portion of the population. For instance, data shows that countries such as the United States have approximately 2 million individuals living with limb loss, with the majority caused by vascular diseases such as diabetes (54 %) and traumatic events (2 %).⁽³⁾

In many countries, the prevalence of transfemoral amputations remains a public health concern. Transfemoral amputations account for a substantial portion of total amputations, ranging between 31 % and 48 % of all amputations, with transtibial amputations making up another 45 %.⁽⁴⁾ Furthermore, individuals with transfemoral amputations face complex rehabilitation challenges, with higher energy expenditure required for mobility, making it critical to provide them with appropriate prosthetic solutions. Countries such as Colombia have been particularly affected due to causes like landmines and conflict, leading to a significant number of transfemoral amputees.⁽³⁾

In Ecuador, the demand for lower-limb prostheses is growing, with centers such as the Fundación Prótesis Imbabura being pivotal in helping amputees regain functionality. Despite this, the lack of immediate access to prosthetic care and rehabilitation continues to be a barrier, especially in low-resource settings. The challenge remains to improve access and ensure timely prosthetic fitting, as early intervention has been associated with improved quality of life for amputees.⁽⁴⁾

Model-based adaptive controllers have emerged as a robust method to ensure stable walking in real-world environments. Azimi et al.⁽⁵⁾ presented a model-based adaptive control system that uses Lyapunov stability to ensure convergence to desired walking gaits. This system was tested in both simulations and outdoor environments, showing significant stability in walking on slopes and uneven terrain.

Gao et al.⁽⁶⁾ introduced a robotic prosthesis with an electrohydraulic knee and motor-driven ankle. This system adjusts impedance in real-time based on ground reaction forces, improving gait symmetry and reducing energy consumption. It was tested successfully in a variety of terrains, including stairs and uneven ground. Similarly, Lawson et al. developed a hybrid control system that combined impedance control during stance phases with trajectory tracking during swing phases, demonstrating efficient level walking with transfemoral amputees.⁽⁷⁾

Zhao et al.⁽⁸⁾ implemented a nonlinear optimization-based controller to enhance energy efficiency and gait tracking. This system dynamically adjusted the control of powered prostheses using real-time data from inertial measurement units (IMUs), achieving smooth transitions between walking states. The same group extended this approach to integrate control Lyapunov functions into the optimization, yielding improved stability in real-world prosthetic walking scenarios.⁽⁹⁾

Sliding mode control has also been explored to address the challenges of gait stability and energy efficiency. Bavarsad et al.⁽¹⁰⁾ proposed a sliding mode controller that optimized energy consumption while enhancing robustness against disturbances and parameter uncertainties, achieving high tracking accuracy for knee and ankle joints. Another study compared sliding mode controllers with traditional PD controllers, showing superior performance in energy efficiency and gait stability in powered prosthetics.⁽¹¹⁾

Several recent studies have proposed finite-state-based controllers to coordinate prosthetic movements with the user's intent. Gao et al. developed a knee-ankle prosthesis that utilized a finite-state controller to adapt to different terrains. The system achieved significant improvements in gait adaptation, with subjects able to walk smoothly on slopes and stairs.⁽¹²⁾

Optimizing control strategies through real-time feedback has become a key focus. Sup et al.⁽¹³⁾ developed a powered knee and ankle prosthesis with an optimization-based controller that enhanced user walking ability. This system adjusted the prosthetic response based on user movement and ground reaction forces, significantly improving gait stability.

Advances in human-inspired control have contributed to smoother gait patterns. Azimi et al.⁽¹⁴⁾ applied human-inspired control systems to power transfemoral prostheses, combining optimization with model-based approaches to generate human-like walking trajectories. Experimental results showed the ability of these systems to mimic natural gait patterns on various terrains.

Energy-efficient controllers remain a top priority in recent research. Bavarsad et al.⁽¹⁵⁾ introduced a state-dependent Riccati equation controller that optimized energy consumption by reducing control effort and improving robustness against disturbances. Similarly, Azimi et al.⁽¹⁶⁾ designed robust controllers that showed significant improvements in tracking performance and energy efficiency when tested on the AMPRO3 prosthesis.

New designs in electromechanical systems have led to more responsive and reliable prosthetic devices. Laschowski et al.⁽¹⁷⁾ reviewed the integration of actuators and sensors into prostheses, highlighting improvements in energy regeneration and the use of bio-inspired sensors for control feedback. These electromechanical advancements have also enabled more accurate control of powered prosthetic limbs.⁽¹⁸⁾

Simulation has played a critical role in testing and refining control systems. Richter et al.⁽¹⁹⁾ developed a robotic testbed for evaluating control systems before human trials. This approach allowed for safe and repeatable testing, facilitating the refinement of control algorithms for better gait performance.

Another significant advancement has been the development of control systems that integrate whole-body awareness. Parri et al.⁽²⁰⁾ introduced a novel control system that used sensors distributed across the body to detect user intent and control prosthetic movements, achieving a high level of accuracy in tasks such as stair climbing and walking.

Lastly, recent work has focused on the application of advanced control systems in rehabilitation environments. Sun et al.⁽²¹⁾ designed a robotic knee-ankle system that assists in rehabilitation by dynamically adjusting to the user's needs. This system significantly improved the rehabilitation outcomes for transfemoral amputees.

METHOD

The robotics transfemoral prosthesis have been developed using model-based design techniques defining different models of the system in order to obtain the system behavior and experiment on it using model-in-the-loop.⁽²²⁾

Figure 1 shows the architecture of the Robotic Transfemoral Prosthesis based on the Mechatronics System Structure.⁽²²⁾ The system is composed of the prosthetics limb which includes the thigh, knee joint and the leg; the accelerometer measures the position of the prosthetics limb and sends it to the physical controller of the system.

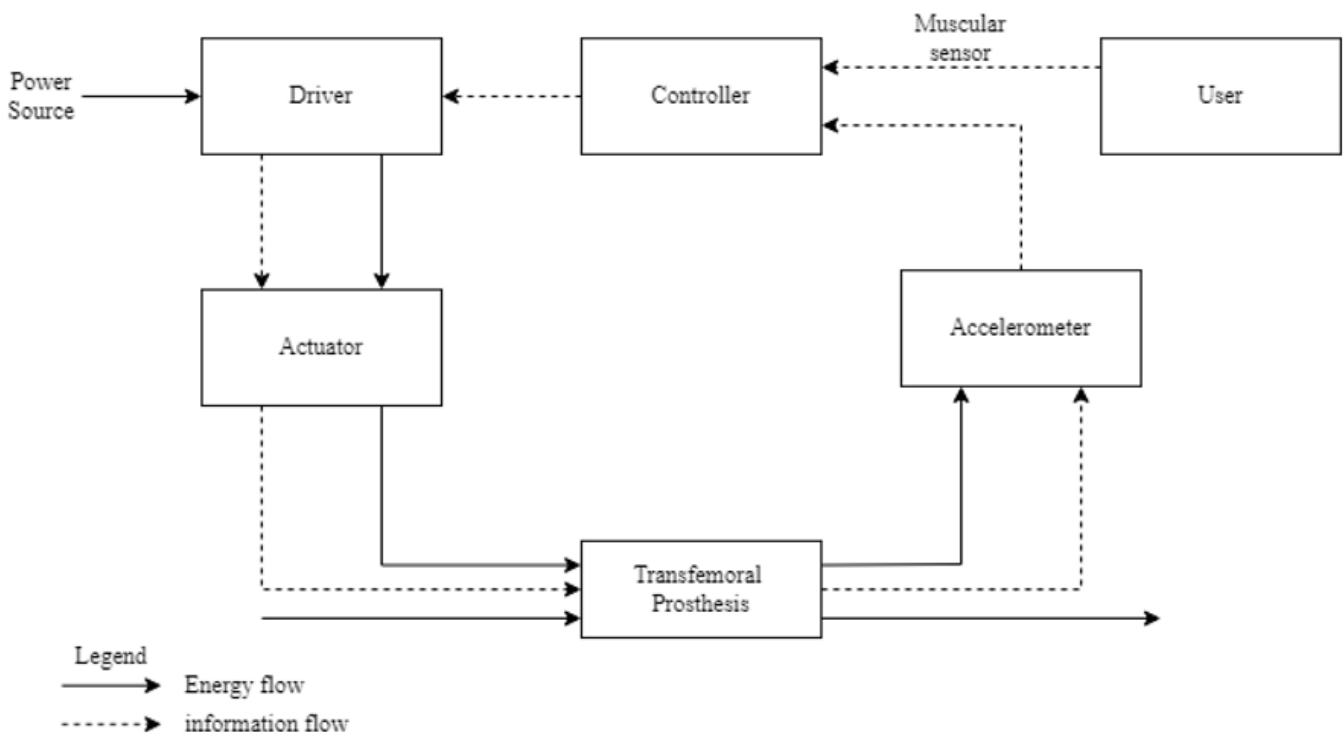


Figure 1. Robotic Transfemoral Prosthesis Architecture⁽²³⁾

It can also be seen that the user communicates to the transfemoral prosthesis by means of a muscular sensor; then the controller analysis both signals, from muscular sensor and accelerometer, and determines the control action, which is sent to the actuator; the latter produces the movement on the prosthetics limb.

For this study the following controllers were chosen to be designed and prove them on the robotic transfemoral prosthesis:

- **Proportional-Derivative (PD) Controller:** the PD controller is a widely used control system that determines the control action by calculating the proportional and derivative of the error between the desired and actual position. The proportional component reduces the magnitude of the error, while the derivative component predicts future errors based on the rate of change.⁽²⁴⁾
- **Feedforward-Feedback PD Controller (FF-FB PD):** the feedforward-feedback PD controller is an extension of the traditional PD control that integrates a feedforward component. The feedforward term anticipates the required control effort based on the reference trajectory, allowing for faster response times. The feedback loop corrects any remaining error, improving the overall performance of the system.⁽²⁵⁾
- **Linear Quadratic Regulator (LQR) Controller:** the LQR controller is an optimal control strategy that minimizes a predefined cost function, balancing the trade-off between minimizing control error and reducing control effort. This state-space controller computes an optimal gain matrix that provides the best possible control inputs for a system.⁽²⁶⁾
- **Feedforward-Feedback LQR Controller (FF-FB LQR):** similar to the feedforward-feedback PD approach, the feedforward-feedback LQR controller incorporates a feedforward term into the LQR framework. This controller uses the LQR's optimal control logic while adding a predictive feedforward component to improve the system's response to desired trajectories.⁽²⁷⁾

The prototype of the robotic transfemoral prosthesis was modeled using CAD (Computer Assisted Design) software and then imported into a simulation software to submit it under test.

To conduct the experiments the four controllers were tested using inputs such as a unit step input and a trajectory that describes flexion leg movement. To assess the controllers' performance the following information was documented.

Step Response Analysis: overshoot, settling time, and steady-state error were measured in response to a unit step input.

Trajectory Tracking: the accuracy in following a motion trajectory over time, steady state error and the amount of torque (in Newton-meters) required to achieve the desired movement were measured. A jerk signal is used to produce the trajectory, which is shown in figure 2.

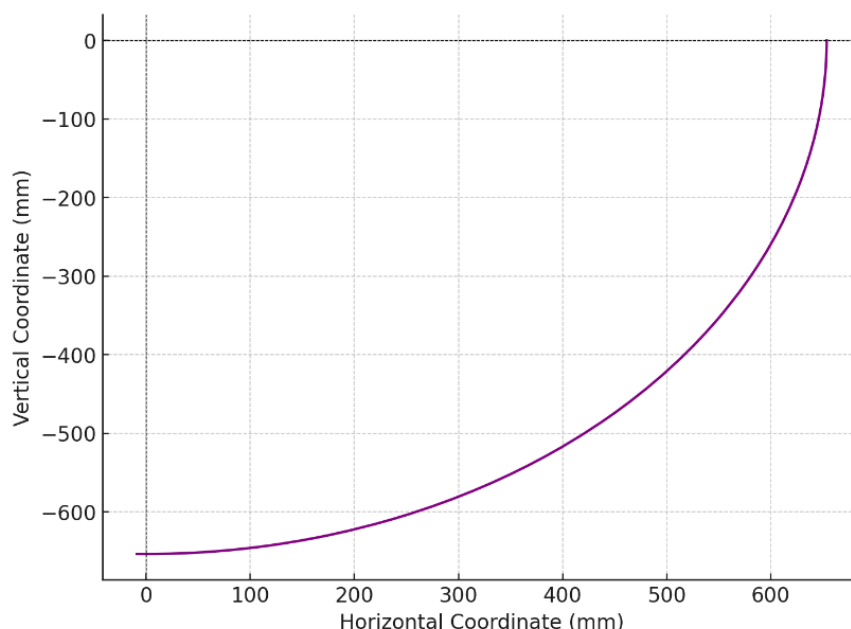


Figure 2. Reference Trajectory

DEVELOPMENT

Figure 3 the diagram of the Robotic Prosthesis. It shows the physical properties considered to develop a mathematical model. This system can be model as a simple pendulum, since the socket stays fixed, while the prosthetic leg moves around the knee. The angular displacement is denoted by the angle θ .

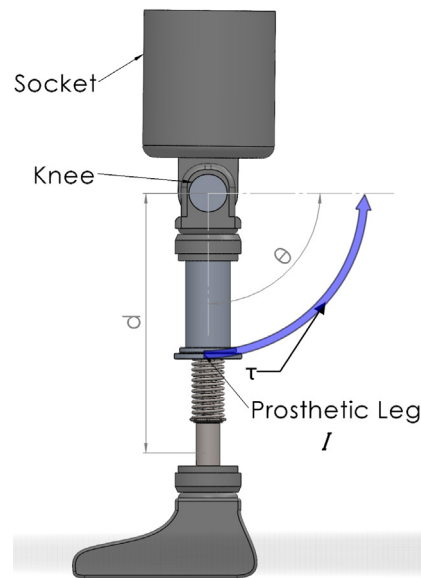


Figure 3. Prosthesis Diagram

Equation (1) represents the equation of motion of the system, which is the result of applying the Euler-Lagrange formalism:

$$I\ddot{\theta} - mgd \sin \theta = \tau \quad (1)$$

Where:

I = moment of inertia of the pylon.

m = mass of the pylon.

d = distance from the pivot to the pylon of the center of mass.

τ = applied torque.

θ = Prosthetic leg angular displacement.

g = gravity acceleration.

Figure 4 illustrates the robotic transfemoral prosthesis in the simulation environment. For this experiment the thigh is attached to a reference system; therefore, the leg moves with respect to the thigh through the knee joint.

On the knee joint the input is applied and the data such as position and required torque are measured.

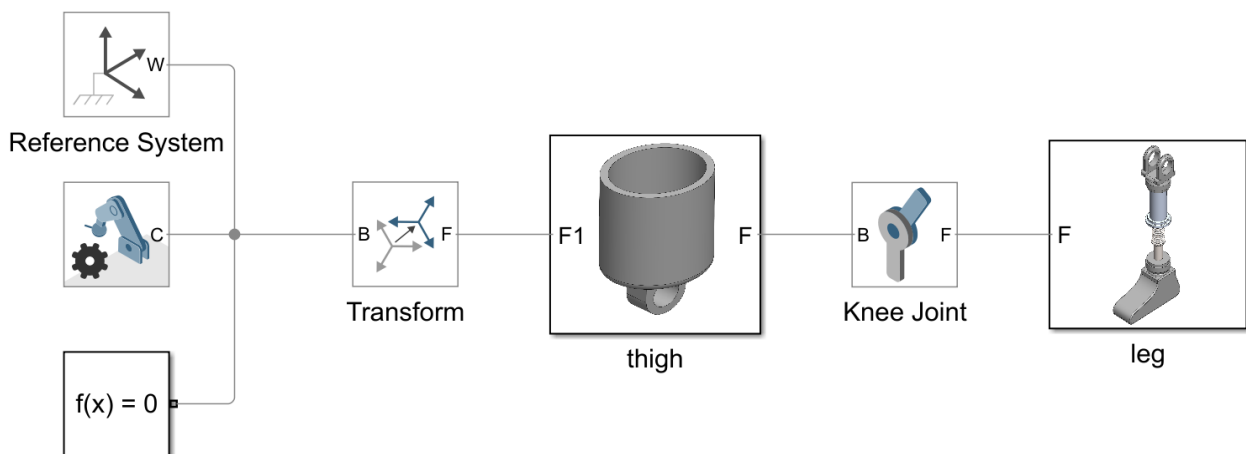


Figure 4. Transfemoral Prosthesis in simulation environment

Controller implementation

The four controllers: PD; feedforward-feedback PD; LQR and feedforward-feedback LQR, were implemented in the simulation environment as presented in the following figures.

PD Controller

Figure 5 shows the PD controller classical structure showing error calculation which is minimized by the PD controller.

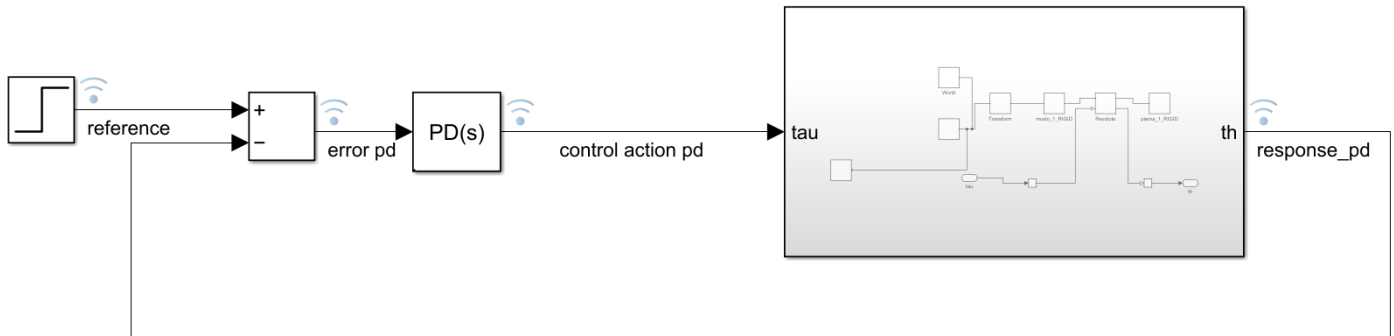


Figure 5. PD Controller Implementation

The controller mathematical representation is presented in equation (2)

$$u(t) = K_p e(t) + K_d \dot{e}(t) \quad (2)$$

The parameters used to tune the controller were $K_p = 565,51$ and $K_d = 47,02$.

Feedforward-Feedback PD Controller

Figure 6 illustrates the implementation of the feedforward-feedback PD controller. The key difference from the regular PD controller is the addition of a feedforward loop.

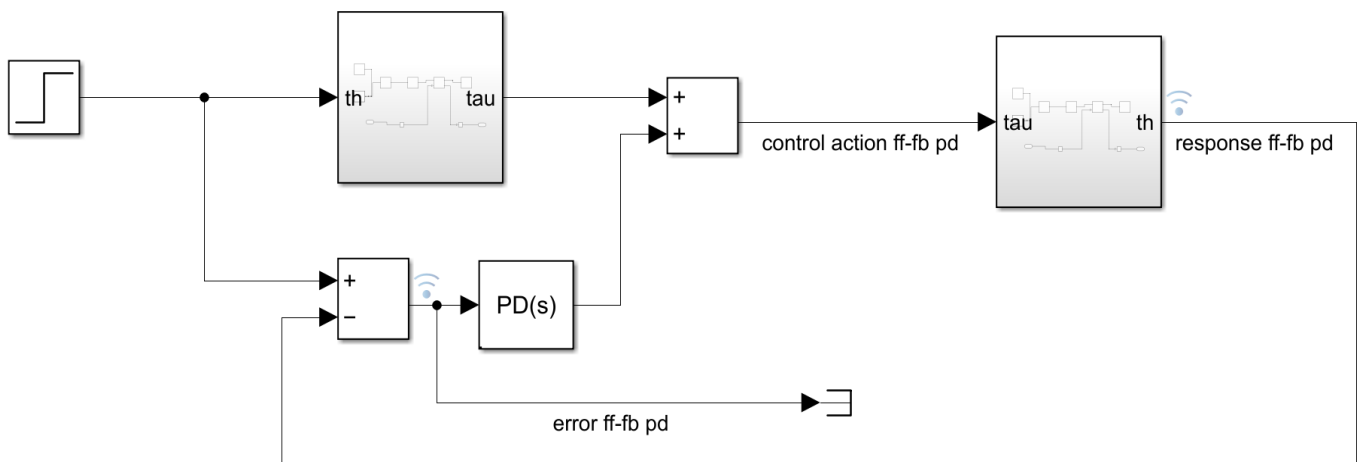


Figure 6. Feedforward - Feedback PD Controller Implementation

The unit step input is fed into the dynamic model of the prosthesis and used to calculate the necessary torque to reach the desired position. This torque and the controller output are added to obtain control action presented in equation (3).

$$u(t) = u_{ff}(t) + K_p e(t) + K_d \dot{e}(t) \quad (3)$$

For this case the tune parameters are: K_p : 672,85 and K_d : 47,02.

LQR Controller

Figure 7 displays the implementation of the LQR controller. The reference signal is scaled by a feedforward gain (K_r) before being compared to the actual position of the prosthetic limb, generating an error signal. This error signal is used to calculate the optimal control action based on the state feedback. The LQR controller minimizes a predefined cost function by using the feedback gain (K^*u) to balance control accuracy and effort.

The resulting control action is applied to the system, and the output is fed back to continuously adjust the control, ensuring precise trajectory tracking while optimizing energy usage.

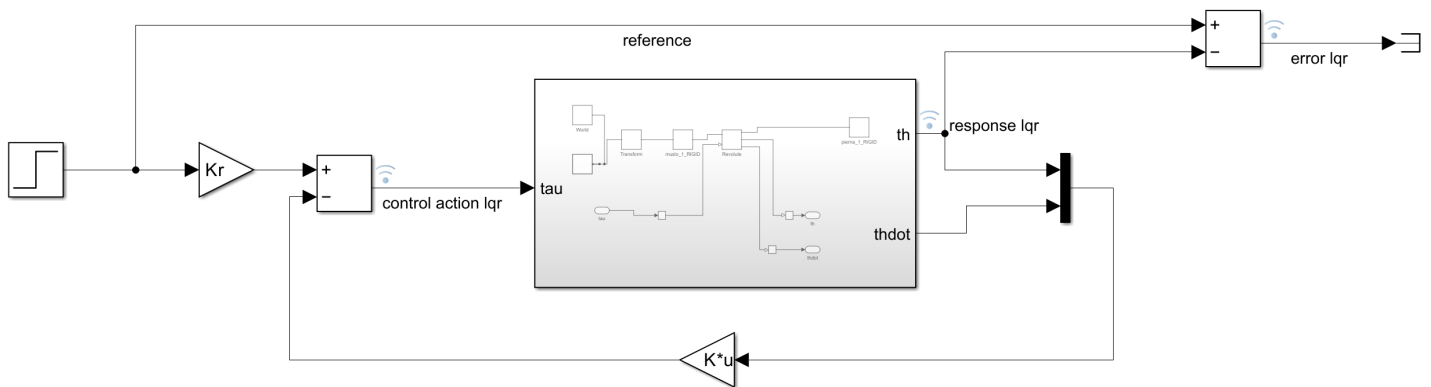


Figure 7. LQR Controller Implementation

Tuning of this controller was developed using the state-space representation which also validates the physical model used in all the experiments. The resulting state-space model is the following:

$$\begin{bmatrix} \dot{x}_1(t) \\ \dot{x}_2(t) \end{bmatrix} = \begin{bmatrix} 0 & 1 \\ -1494 & -54.63 \end{bmatrix} \begin{bmatrix} x_1(t) \\ x_2(t) \end{bmatrix} + \begin{bmatrix} 0 \\ 1494 \end{bmatrix} u$$

$$\begin{bmatrix} y_1(t) \\ y_2(t) \end{bmatrix} = \begin{bmatrix} 1 & 0 \end{bmatrix} \begin{bmatrix} x_1(t) \\ x_2(t) \end{bmatrix}$$

The controller mathematical expression is presented in equation (4):

$$u(t) = K_r x_{ref}(t) - Kx(t) \quad (4)$$

The constants obtained for the LQR controller are: $K = [991, 39; 36, 57]$ and $K_r = 1000$.

Feedforward-Feedback LQR Controller

Figure 8 shows the feedforward-feedback LQR controller, which combines both feedforward and feedback strategies for optimal control. The feedforward path, scaled by the gain (K_r), allows the system to anticipate control actions based on the reference input. Simultaneously, the feedback loop, using state feedback with the gain ($K \cdot u$), ensures that the system continuously adjusts the control action to minimize the error between the reference and the actual system state. The combined control action is applied to the system, with the feedback loop further refining performance to improve accuracy and reduce error during dynamic movements. For this case the same constants used in the LQR controller worked for this one.

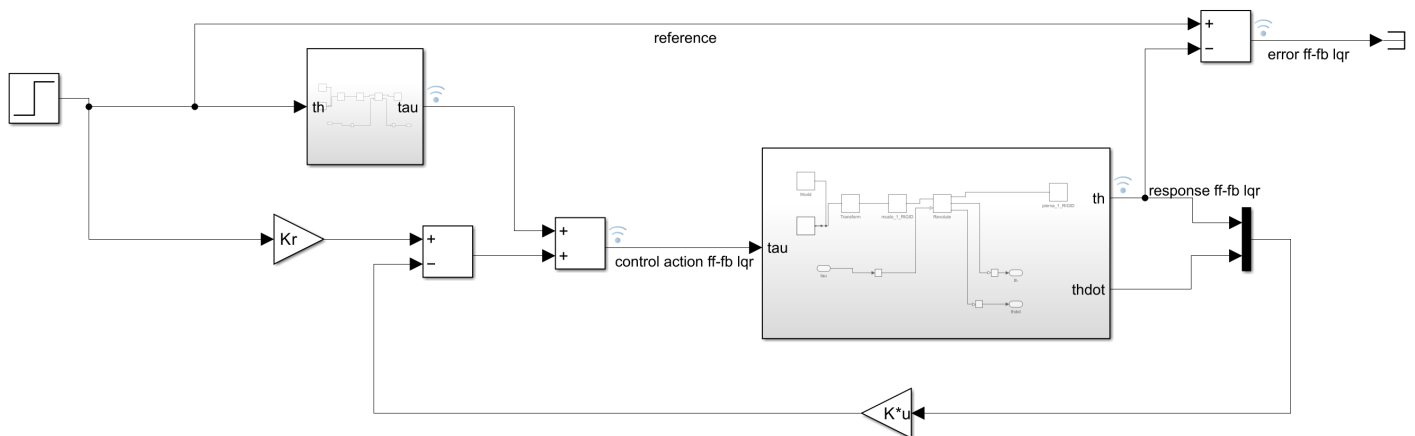


Figure 8. Feedforward-Feedback LQR Implementation

This controller is presented in equation (5).

$$u(t) = u_{ff}(t) + K_r x_{ref}(t) - Kx(t) \quad (5)$$

All the tests were executed under the same conditions. The leg starts extended and then it reaches its final position. A on second interval was used to obtain the step response. In the case of the trajectory input, the simulations lasted ten seconds. Also, all the gravity is considered for all the tests. In the previous figures, only the step input is shown; however, in all controllers this input was replaced with a flexion trajectory.

RESULTS

The step responses for four control methods, namely PD, LQR, FF-FB PD, and FF-FB LQR, were analyzed to evaluate system performance in terms of overshoot and time to reach stability.

The PD control exhibited an overshoot of 10,06 %, while the FeedForward-Feedback PD control reached an overshoot of 11,96 %. The LQR method produced an overshoot of 4,22 %. Both feedforward-feedback. The FeedForward-Feedback LQR control demonstrated the best performance, with an overshoot of 4,98 %.

Overall, the FeedForward-Feedback methods, particularly FeedForward-FeedbackLQR, outperformed the standard PD and LQR methods by providing smaller overshoots. Considering the 2 % threshold tolerance for the settling time, the PD Controller stabilized at 0,164 seconds while its FF-FB PD Controller version took 0,178 seconds. For the LQR Controller the settling time was 0,187 seconds and for the FF-FB LQR Controller was 0,187 seconds.

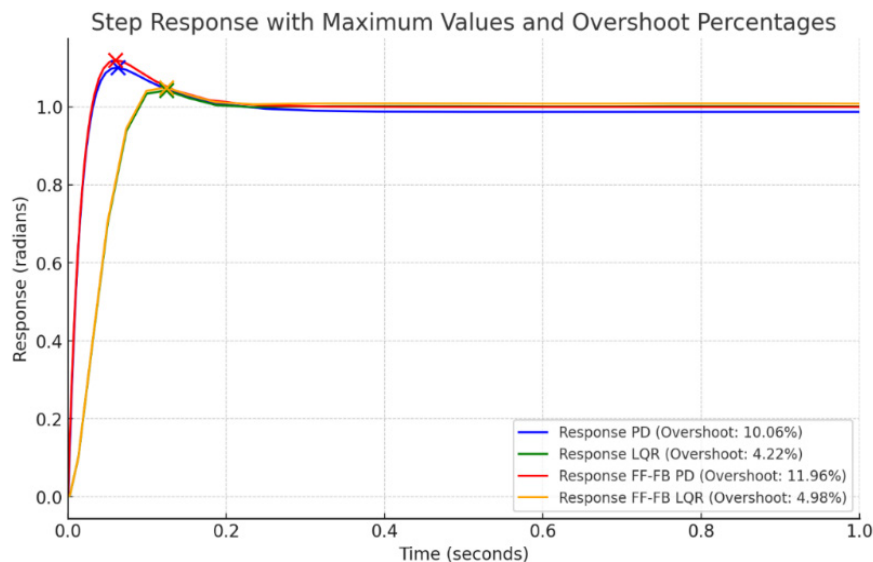


Figure 9. Prosthesis Step response

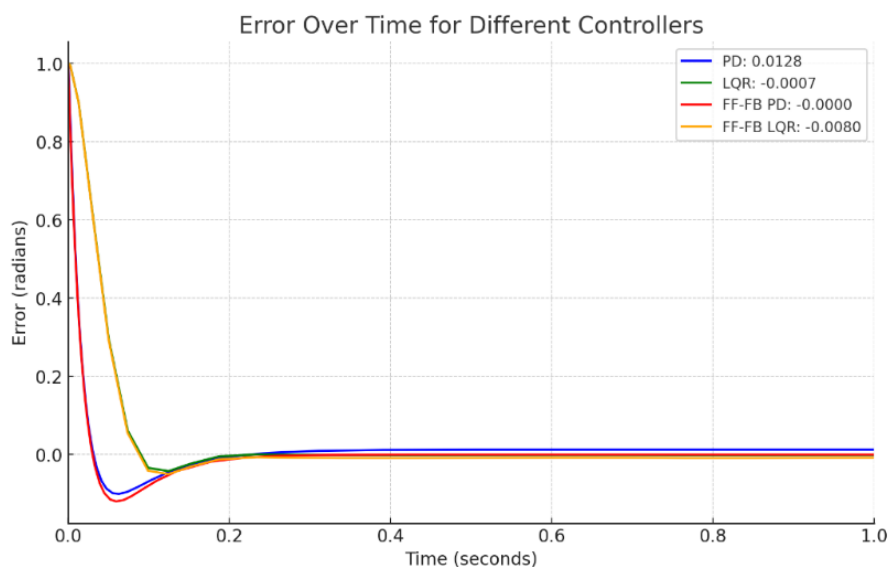


Figure 10. Error over time

Figure 10 presents the error response over time for four control strategies. All controllers minimize the error within the first 0,2 seconds, after which the error stabilizes. The PD controller exhibits a steady-state error of approximately 0,0128 radians, while the LQR controller achieves a steady-state error of 0,0007 radians. The FF-FB PD controller reduces the error further, reaching $1,14 \times 10^{-8}$ radians which is practically 0. The LQR controller shows an error of 0,0007 radians while the FF-FB LQR controller shows a steady-state error of 0,0080 radians.

Figure 11 depicts the trajectory response for the four control strategies compared to a reference trajectory, represented by the dashed black line. All controllers attempt to track the reference almost accurately. The LQR and FF-FB PD controllers exhibit the closest tracking to the reference with minimal deviation. The LQR and PD controllers show larger deviations compared to the other two strategies; however, they still show good tracking performance.

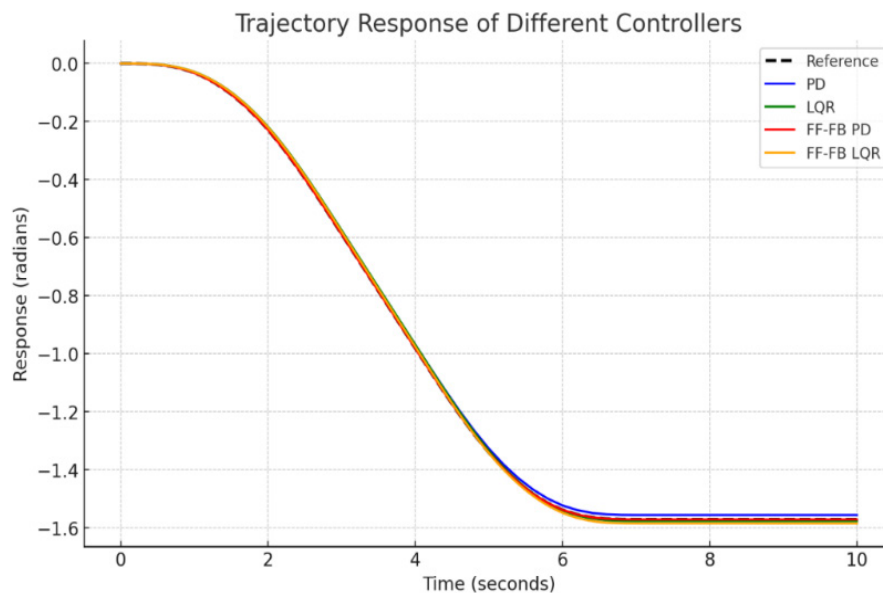


Figure 11. Trajectory Response

Figure 12 shows the control action in terms of the required torque measured in N.m. All the controllers need approximately 8,6 Nm to reach the final position.

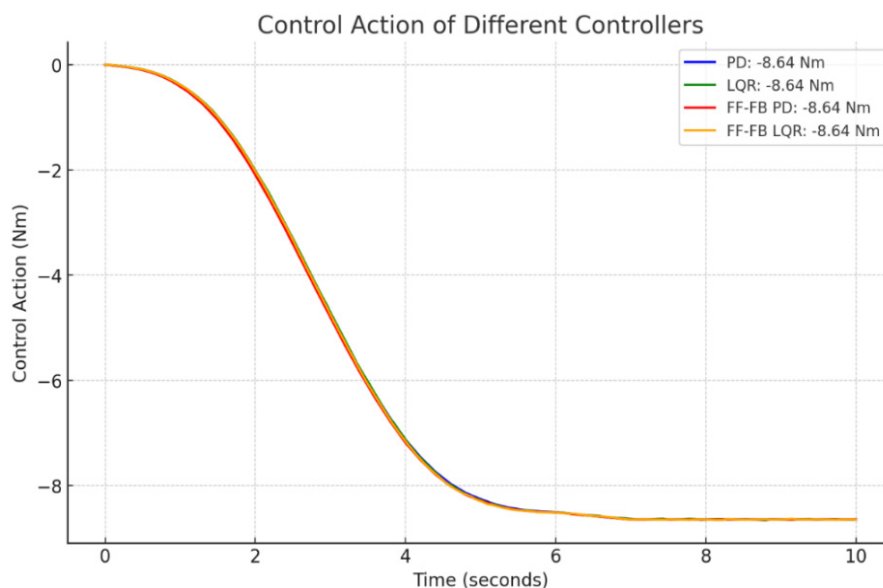


Figure 12. Control Action for the Trajectory Tracking

Figure 13 presents the trajectory error over time for four control strategies. The LQR and FF-FB PD controllers demonstrate the smallest tracking errors. The FF-FB LQR and PD controllers show larger errors compared to the other two controllers even though their values are quite small.

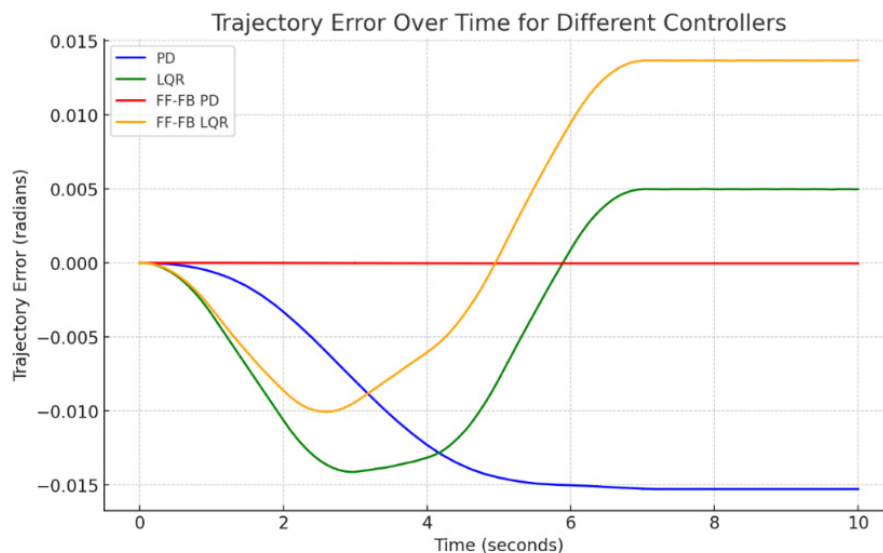


Figure 13. Trajectory Tracking Error

DISCUSSION

This study compared the performance of four controllers—PD, FF-FB PD, LQR, and FF-FB LQR—in controlling a robotic transfemoral prosthesis. Key performance metrics such as overshoot, settling time, trajectory tracking accuracy, and torque requirements were evaluated, providing insights into the strengths and limitations of each control strategy.

All four controllers required approximately 8,6 Nm to reach the desired position for trajectory tracking. This indicates that despite the differences in control algorithms, the mechanical effort to move the prosthesis was similar across the board. This could suggest that while different control strategies offer varied performance in terms of accuracy and stability, the overall energy required to perform the motion remains consistent.

The LQR controller exhibited the lowest overshoot during the step response, with just 4,22 %, while the PD-based controllers had higher overshoot values. The FF-FB PD controller showed the highest overshoot at 11,96 %. Although the FF-FB LQR controller had a slightly higher overshoot than the LQR controller, both performed within an acceptable range and demonstrated better control of stability compared to the PD and FF-FB PD controllers. This finding suggests that LQR-based controllers, particularly the FF-FB LQR, provide superior performance in maintaining stability and minimizing overshoot.

In terms of trajectory tracking, the FF-FB PD controller reduced the error to nearly zero, outperforming the other controllers in this metric. The LQR and FF-FB LQR controllers, while demonstrating some deviation from the reference trajectory, still exhibited strong tracking performance. On the other hand, the PD controller had the largest deviation, indicating that it may not be ideal for applications requiring high precision in movement tracking. These results highlight the potential of feedforward-feedback control strategies, particularly when trajectory accuracy is critical.

CONCLUSIONS

The feedforward-feedback LQR controller demonstrated the best overall performance in terms of stability, overshoot, and trajectory tracking accuracy, making it a superior choice for controlling robotic transfemoral prostheses. It successfully minimized overshoot and provided accurate trajectory tracking compared to other controllers.

Despite the differences in control strategies, all controllers required a similar amount of torque (~8,6 Nm) to execute the prosthesis movement. This suggests that while control accuracy and stability vary between methods, the mechanical effort needed to achieve the desired movement remains relatively consistent.

BIBLIOGRAPHIC REFERENCES

1. Consejo Nacional para la Igualdad de Discapacidades-CONADIS. Registro Nacional de Discapacidades. Total de personas con discapacidad registradas. 2023.
2. (WHO) World Health Organization. Assistive devices and prosthetics: World report on disability. 2019.
3. Pozo G. Evaluación Pre y Post Protésica en Pacientes de la Fundación Imbabura. Universidad Técnica del Norte; 2020.

4. Benavidez A, Molina R. Estrategias de Evaluación para la Amputación Transfemoral: Revisión Sistemática. 2020.
5. Azimi V, Shu T, Zhao H, Gehlhar R, Simon D, Ames A. Model-Based Adaptive Control of Transfemoral Prostheses: Theory, Simulation, and Experiments. *IEEE Trans Syst Man Cybern Syst.* 2019;51:1174-91.
6. Gao X, Si J, Wen Y, Li M, Huang H. Knowledge-Guided Reinforcement Learning Control for Robotic Lower Limb Prosthesis. In: 2020 IEEE International Conference on Robotics and Automation (ICRA). 2020. p. 754-60.
7. Lawson B, Mitchell JE, Truex D, Shultz A, Ledoux ED, Goldfarb M. A Robotic Leg Prosthesis: Design, Control, and Implementation. *IEEE Robot Autom Mag.* 2014;21:70-81.
8. Zhao H, Horn J, Reher J, Paredes V, Ames A. First steps toward translating robotic walking to prostheses: a nonlinear optimization based control approach. *Auton Robots.* 2017;41:725-42.
9. Zhao H, Reher J, Horn J, Paredes V, Ames A. Realization of nonlinear real-time optimization based controllers on self-contained transfemoral prosthesis. In: Proceedings of the ACM/IEEE Sixth International Conference on Cyber-Physical Systems. 2015.
10. Bavarsad A, Fakharian A, Menhaj M. Optimal Sliding Mode Controller for an Active Transfemoral Prosthesis Using State-Dependent Riccati Equation Approach. *Arab J Sci Eng.* 2020;1-14.
11. Azimi V, Simon D, Richter H, Fakoorian S. Robust composite adaptive transfemoral prosthesis control with non-scalar boundary layer trajectories. In: American Control Conference (ACC). 2016. p. 3002-7.
12. Gao S, Wang C, Zhu J, Mai J, Wang Q. Hydraulic Damping and Swing Assistance Control of A Robotic Electrohydraulic Transfemoral Prosthesis: Preliminary Results. 2019 IEEE International Conference on Advanced Robotics and its Social Impacts (ARSO). 2019;365-8.
13. Sup F, Bohara A, Goldfarb M. Design and Control of a Powered Transfemoral Prosthesis. *Int J Rob Res.* 2008;27:263-73.
14. Azimi V, Shu T, Zhao H, Gehlhar R, Simon D, Ames A. Model-Based Adaptive Control of Transfemoral Prostheses: Theory, Simulation, and Experiments. *IEEE Trans Syst Man Cybern Syst.* 2019;51:1174-91.
15. Bavarsad A, Fakharian A, Menhaj M. A nonlinear robust optimal controller for an active transfemoral prosthesis: An estimator-based state-dependent Riccati equation approach. *Proceedings of the Institution of Mechanical Engineers, Part I: Journal of Systems and Control Engineering.* 2020;235:313-29.
16. Azimi V, Fakoorian S, Nguyen T, Simon D. Robust Adaptive Impedance Control With Application to a Transfemoral Prosthesis and Test Robot. *J Dyn Syst Meas Control.* 2018;
17. Laschowski B, Andrysek J. Electromechanical Design of Robotic Transfemoral Prostheses. Volume 5A: 42nd Mechanisms and Robotics Conference. 2018;
18. Richter H, Simon D, Smith WA, Samorezov S. Dynamic Modeling, Parameter Estimation and Control of a Leg Prosthesis Test Robot. *Appl Math Model.* 2015;39:559-73.
19. Richter H, Hui X, Bogert AJ, Simon D. Semiactive virtual control of a hydraulic prosthetic knee. 2016 IEEE Conference on Control Applications (CCA). 2016;422-9.
20. Parri A, Martini E, Geeroms J, Flynn L, Pasquini G, Crea S, et al. Whole Body Awareness for Controlling a Robotic Transfemoral Prosthesis. *Front Neurobot.* 2017;11.
21. Sun X, Sugai F, Okada K, Inaba M. Design and Control of a Novel Robotic Knee-Ankle Prosthesis System. 2018 7th IEEE International Conference on Biomedical Robotics and Biomechatronics (Biorob). 2018;737-43.
22. Ingenieurere Verein Deutscher. Entwicklungsmethodik für mechatronische Systeme Design methodology for mechatronic systems VDI 2206. Design. 2004. 118 p.

23. Vergara S, Mosquera Canchingre G, Bonilla V, Rueda-Ayala C, Hidalgo L. Diseño mecánico de una prótesis transfemoral. Avances y desafíos en las ciencias y la ingeniería 2023: nuevos conocimientos para un futuro sostenible [Internet]. 2023 [cited 2024 Sep 25];122. Available from: https://www.researchgate.net/profile/Hector-Rojas-14/publication/373762565_Bioeconomia_y_desarrollo_territorial_en_Narino_Tolima_Guajira_y_Bogota-Region_aproximacion_desde_la_triple_helice/links/653f0c253cc79d48c5ba020e/Bioeconomia-y-desarrollo-territorial-en-Narino-Tolima-Guajira-y-Bogota-Region-aproximacion-desde-la-triple-helice.pdf#page=122

24. Astrom KJ, Murray RM. Feedback systems: An introduction for scientists and engineers [Internet]. Princeton, NJ: Princeton University Press; 2012. Available from: https://consensus.app/papers/feedback-systems-introduction-scientists-engineers-karl-astrom/8ccfef64d31bcd563c7637ecfcb88e69/?utm_source=chatgpt

25. Nise NS. Control systems engineering [Internet]. 6th ed. Hoboken, NJ: Wiley; 2011. Available from: https://consensus.app/papers/control-systems-engineering-norman-s-nise/60348f7fbfa674120c9cb39c5e7335e3/?utm_source=chatgpt

26. Anderson BDO, Moore JB. Optimal control: Linear quadratic methods [Internet]. Mineola, NY: Dover Publications; 2007. Available from: https://consensus.app/papers/optimal-control-linear-quadratic-methods-anderson/b77d422ae8be79940ffcbace35d44ec5/?utm_source=chatgpt

27. Franklin GF, Powell JD, Emami-Naeini A. Feedback control of dynamic systems [Internet]. 8th ed. Upper Saddle River, NJ: Pearson; 2019. Available from: https://consensus.app/papers/feedback-control-dynamic-systems-franklin/70fb517e98a5a57b8dc89ad580f6c785/?utm_source=chatgpt

FINANCING

No financing.

CONFLICT OF INTEREST

The authors declare that there is no conflict of interest.

AUTHORSHIP CONTRIBUTION

Conceptualization: Guillermo Mosquera, Vladimir Bonilla, Sofía Vergara.

Data curation: Guillermo Mosquera, Vladimir Bonilla.

Formal analysis: Guillermo Mosquera, Christian Rueda, Marcelo Moya.

Research: Guillermo Mosquera, Vladimir Bonilla, Sofía Vergara.

Methodology: Guillermo Mosquera, Vladimir Bonilla.

Project management: Guillermo Mosquera.

Resources: Guillermo Mosquera, Vladimir Bonilla, Sofía Vergara, Christian Rueda, Marcelo Moya.

Software: Guillermo Mosquera, Vladimir Bonilla.

Supervision: Sofía Vergara.

Validation: Christian Rueda, Marcelo Moya.

Display: Guillermo Mosquera, Vladimir Bonilla, Christian Rueda.

Drafting - original draft: Guillermo Mosquera, Vladimir Bonilla, Sofía Vergara, Christian Rueda, Marcelo Moya.

Writing - proofreading and editing: Guillermo Mosquera, Vladimir Bonilla, Sofía Vergara, Christian Rueda, Marcelo Moya.